Perceived realism of virtual textures rendered by a vibrotactile wearable ring display

Friesen, Rebecca Fenton; Vardar, Yasemin

DOI
10.1109/TOH.2023.3304899

Publication date
2024

Document Version
Final published version

Published in
IEEE Transactions on Haptics

Perceived Realism of Virtual Textures Rendered by a Vibrotactile Wearable Ring Display

Rebecca Fenton Friesen, *Member, IEEE*, and Yasemin Vardar, *Member, IEEE*

***Abstract*—Wearable haptic displays that relocate feedback away from the fingertip provide a much-needed sense of touch to interactions in virtual reality, while also leaving the fingertip free from occlusion for augmented reality tasks. However, the impact of relocation on perceptual sensitivity to dynamic changes in actuation during active movement remains unclear. In this work, we investigate the perceived realism of virtual textures rendered via vibrations relocated to the base of the index finger and compare three different methods of modulating vibrations with active finger speed. For the first two methods, changing finger speed induced proportional changes in either frequency or amplitude of vibration, and for the third method did not modulate vibration. In psychophysical experiments, participants compared different types of modulation to each other, as well as to real 3D-printed textured surfaces. Results suggest that frequency modulation results in more realistic sensations for coarser textures, whereas participants were less discerning of modulation type for finer textures. Additionally, we presented virtual textures either fully virtually in midair or under augmented reality in which the finger contacted a flat surface; while we found no difference in experimental performance, participants were divided by a strong preference for either the contact or non-contact condition.**

***Index Terms*—Surface haptics, texture, wearables, virtual reality.**

I. Introduction

RECENT advances in virtual reality interfaces allow us to explore immersive virtual worlds and complex objects through rich visual and auditory feedback, yet haptic interactions with virtual stimuli remain far more primitive. Commercially available haptic displays attempting to close this gap, such as vibrating handheld controllers [1], [2] or gloves [3], [4], generally provide haptic feedback directly to the fingertips or palm. While these locations are where a user would expect sensations during active touch, such placements can be particularly problematic for augmented and mixed reality: occluding the fingertip with gloves or other hardware demonstrably reduces tactile acuity [5], [6], and bulky hardware concentrated in the small workspace of the hand can hamper dexterity. One approach to mitigate these deleterious effects is to "fold away" actuators when not needed, and apply them to the fingertip only during virtual interactions [7]. An alternative solution is the use of relocated feedback, in which haptic stimulation that would normally occur at the fingertip or hand is permanently relocated to a more convenient location for actuation such as the wrist or proximal parts of the hand, which provides a larger work area and leaves the fingertip free for additional tasks.

Relocated feedback has proven promising for several types of haptic interactions [8], particularly when using squeeze or shear forces as intelligible cues of contact and softness of virtual objects [9], [10], [11]. Of particular interest to us is the relocation of texture-induced vibrations, traditionally applied via a grasped stylus [12], [13], [14] or directly to the fingertip [15], [16], [17] to mimic the sensation of interacting with a textured surface. While the aforementioned works repeatedly demonstrate that people can identify distinct vibration patterns as different textures and are sensitive to changes in frequency, intensity, and spectral complexity, preliminary research [18] is still exploring whether such rich frequency information even remains intelligible when relocated away from the fingertip. Other research groups are focusing primarily on device design of low-profile wearable rings, demonstrating compact methods of actuation, broadband vibratory feedback, and dynamic stimulation for both navigation cues [19] and texture display [20], [21].

A significant challenge when designing small vibrating wearable devices for realistic texture rendering is accounting for the large changes in the frequency content of real texture-induced vibrations as the active finger dynamically moves and changes speed [22]. In order to mimic these real interactions, vibration frequencies must modulate with fingertip speed such that spatial frequencies remain constant [23]. This rendering method often relies on measured position of the finger to preserve spatial constancy of texture patterns [24], with changes to temporal frequency a direct result of changes in speed. However, such implementation results in several practical challenges; firstly, one must account for the strong resonances of many vibrotactile actuators that result in dramatic changes in intensity that couple with any change in frequency [25]. Additionally, preserving spatial frequency requires monitoring finger speed and updating actuator output at a rate much faster than would be necessary

Manuscript received 2 January 2023; revised 6 April 2023 and 25 July 2023; accepted 5 August 2023. Date of publication 14 August 2023; date of current version 20 June 2024. This work was supported by the Delft University of Technology. This paper was recommended for publication by the Guest Editors of the Special Issue on Haptics in the Metaverse. *(Corresponding author: Rebecca Fenton Friesen.)*

This work involved human subjects or animals in its research. Approval of all ethical and experimental procedures and protocols was granted by the Ethics Board of Delft University of Technology (TU Delft) under Application No. 1781, and performed in line with the Declaration of Helsinki.

Rebecca Fenton Friesen is with the Department of Mechanical Engineering, Texas A&M University, College Station, TX 77843 USA, and also with the Department of Cognitive Robotics, Delft University of Technology, 2628 CD Delft, The Netherlands (e-mail: rfriesen@tamu.edu).

Yasemin Vardar is with the Department of Cognitive Robotics, Delft University of Technology, 2628 CD Delft, The Netherlands (e-mail: y.vardar@tudelft.nl).

Digital Object Identifier 10.1109/TOH.2023.3304899

for alternative methods such as amplitude envelope modulation. We hypothesize that for some texture-mimicking vibrations, particularly when relocated to less sensitive areas away from the fingertip, the additional challenges of preserving spatial frequency through continuous variation of temporal frequency may be unnecessary. We ask whether modulating amplitude instead, which still preserves expected changes in spectral power [23], could result in equivalently realistic sensations of texture.

In this study, we explore the impact of several particular velocity-dependent signal modulation schemes on perceived realism and discrimination of virtual textures for a relocated vibrotactile display worn as a ring. Three different modulation types were considered; 1) varying the vibration frequency as finger velocity changed, analogous to maintaining a constant spatial frequency, 2) varying the amplitude of vibration with finger velocity, such that signal power proportionally increases with increasing velocity, and 3) no modulation of vibration at all while the finger is moving, regardless of scanning velocity. We tested these modulation schemes with both fine and coarser (i.e. high and lower frequency) virtual textures, as well as when the finger was or was not receiving additional surface cues via contact with a flat surface. We looked for impacts on judgments of realism and pleasantness of the virtual textures, both in comparison to real textures and compared to each other.

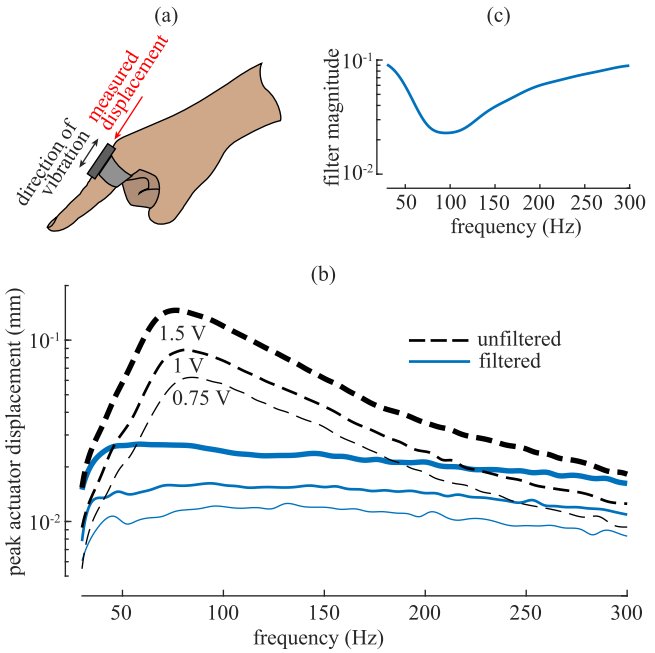

Fig. 1. (a) Placement of the vibrotactile actuator and measurement location of the generated vibrations via laser doppler vibrometer. (b Peak actuator displacement as a function of input frequency for three different input amplitudes. (c) Filter for flattening actuator resonant peak.

II. System Design

The following section details our construction and control of virtual textures applied via a wearable vibrotactile ring. We first present the design and characterization of the wearable ring, as well as the wider experimental apparatus for tracking participant movement and controlling the ring output. We then describe the virtual textures and types of velocity modulation used in this study, and the real textures used for comparison. In the subsequent section, these virtual stimuli and real textures were compared and the impact of modulation type, amplitude, and frequency of virtual textures on perceived realism and pleasantness was assessed in a series of psychophysical experiments.

A. Wearable Ring

Our primary design considerations for the wearable texture ring display were the location, size, and frequency response of the actuator. We chose to locate actuation on the dorsal side of the proximal phalanx of the index finger, as shown in Fig. 1(a), leaving the fingertips and grasp area (i.e. ventral side of the hand) relatively unencumbered yet otherwise keeping actuation close to the fingertip. The actuator used in this study was the HapCoil-One (Tactile Labs), measuring 11x11x37 mm and attached so as to vibrate in the direction along the finger, laterally against the skin. We chose this actuator as it has a stated bandwidth of 10–1000 Hz, spanning the majority of the human tactile perceptual range (0–1000 Hz) [26]. Additionally, it is small enough to fit within the approximately 15x40 mm workspace of an index finger's proximal phalanx. We characterized the actuator behavior using a single-point laser doppler vibrometer (Polytec OFV–5000, OFV–505 sensor head). All measurements aligned with the direction of vibration and were taken while the actuator was in contact with the hand (see Fig. 1(a)). The actuator was secured to the index finger using a Velcro strap with an integrated force sensor (FSR 402, Interlink Electronics) and tightened to apply a 0.5 N squeezing force. The input voltage of the actuator was amplified with a class D audio amplifier, the AudioAmp 2 Click (Mikro Electronika) with 20 dB gain. The HapCoil-One has a reported resonant frequency of 65 Hz, observed in the peak actuator displacement plotted in Fig. 1(b). In order to achieve standardized actuator displacement regardless of commanded frequency, we passed our output voltage through a 400th order zero phase arbitrary response filter, hand-tuned in Matlab 2021 (see Fig. 1(c)).

The addition of the filter considerably flattened the displacement magnitude; the steep roll-off in amplitude below 30 Hz is due to the high pass filtering of the amplifier, necessary to protect the actuator from DC voltage offsets. Performance of the filter was observed at three different base voltage levels, as shown in Fig. 1(b), to demonstrate linearity across multiple amplitudes.

Velocity-dependent haptic rendering requires real-time velocity estimation. In this experiment, we tracked finger position, and therefore velocity, with a one-degree-of-freedom pulley system shown in Fig. 2(a)–(c). The bottom of the wearable ring clipped into a magnetic bracket on the thin nonelastic fishing line stretched between two pulleys and a quadrature encoder shaft. As a user moved their finger back and forth across the texture samples, the encoder provided a resolution of 10.6μm, monitored at 10 kHz.

B. Real Textures

We designed and 3D printed a set of textured surfaces for use in comparison tests with our virtual texture display. The real

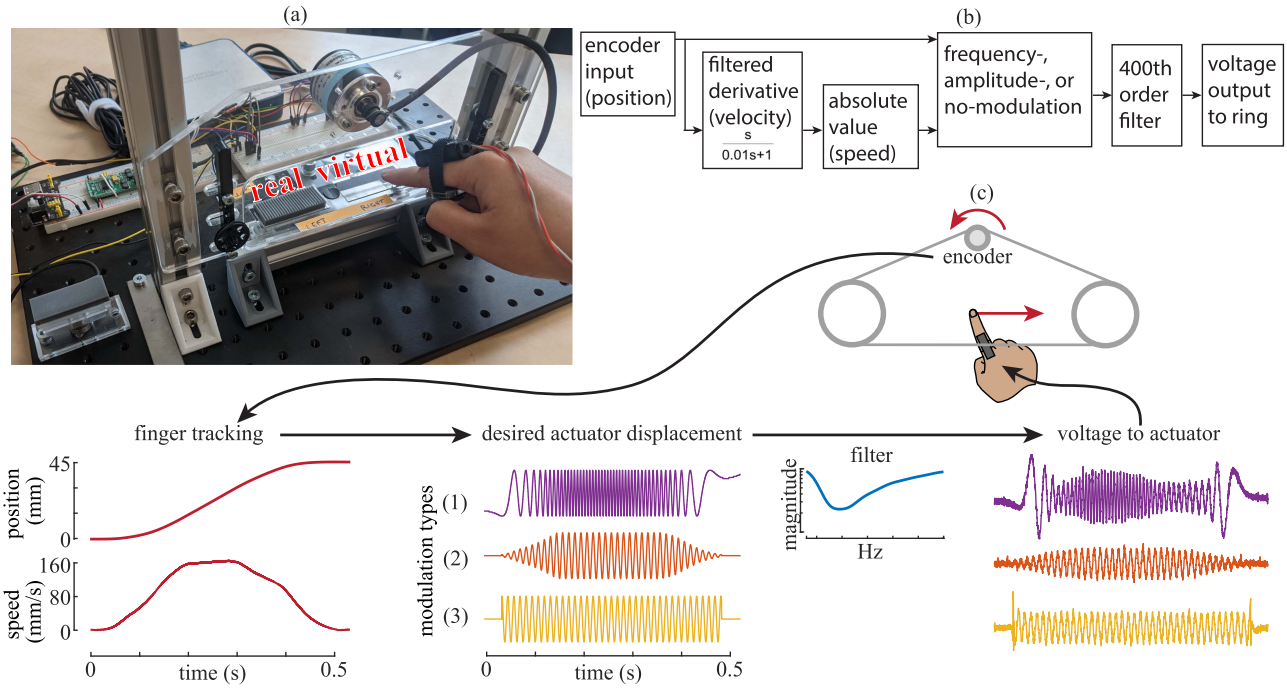

Fig. 2. (a) The experimental setup with a participant feeling both a real and virtual texture side by side. (b) Simplified diagram of Simulink Realtime model, measuring encoder input and generating voltage output at 10 kHz. (c) Pictorial progression of virtual texture rendering. 10 kHz sampled encoder output and its filtered derivative provide position and speed of the finger. Paired with equations (1)-(3), this generates a virtual texture using one of three different modulation types: 1- frequency modulation (FM), 2- amplitude modulation (AM), and 3- no modulation (NM). The desired displacement signal is passed through a 400th order zero phase arbitrary response filter to remove amplification effects of actuator resonance. Finally, the filtered voltage signal is sent to the actuator to produce a vibration with the desired displacement.

textures consisted of 3D printed resin using stereolithography (manufactured by 3Delft), and all had a 20 mm x 50 mm surface area. We deemed the 50 mm length long enough for a user to swipe their finger along, but short enough to fit two textures side by side for comparison in our display.

All textures consisted of a single spatial frequency component that varied along the longest axis. We originally designed textures with a spatial frequency as high as 2 mm^{-1}, or 0.5 mm ridge spacing. However, this spacing proved so fine that it elicited no noticeable vibration on a sliding finger, instead serving only to reduce the overall friction coefficient. We therefore selected real textures coarser than this value, while still fine enough to induce vibrations within the bandwidth of our vibrotactile actuator. The final set consisted of 0.5 mm^{-1}, 1 mm^{-1}, and 1.5 mm^{-1} spatial sinusoids; see Fig. 3 for close-up photos of each texture. All textures had a peak-to-trough height of 1 mm.

In order to ascertain that these textures do elicit vibrations that correspond with their spatial frequency, we measured the lateral force between a finger and the textured surface during active scanning. Textures were mounted on a 6-axis force sensor (ATI Nano17 Titanium), and the first author swiped each sample for 5 seconds with a normal force trained to average 0.4 N and a scanning speed averaging 80 mm/s. Speed was regulated using a metronome, so in practice varied widely as the finger changed direction back and forth across the texture sample. Despite non-precise instantaneous force and speed, all three textures induce the expected vibrations, as can be seen in both the time domain snapshot and summary spectral data in Fig. 3.

C. Virtual Textures

In the context of this study, all virtual textures are vibrations applied to the proximal phalanx of the right index finger during movement, consisting of a single frequency component corresponding to each of the real texture samples. We tested three types of velocity-dependent modulation of virtual textures S_{1-3}:

$$S_1(x,t) = A\sin(2\pi f_s x) = A\sin(2\pi \mathbf{f}(\dot{x})t) \tag{1}$$

$$S_2(x,t) = \mathbf{A}(\dot{x})\sin(2\pi f_{@80} t) \tag{2}$$

$$S_3(x,t) = \begin{cases} A\sin(2\pi f_{@80} t) & |\dot{x}| > 0, \\ 0 & \dot{x} = 0. \end{cases} \tag{3}$$

Here, A, t, x, f_s, f refer to vibration signal amplitude, time, finger displacement in lateral direction, and spatial and temporal frequency of a texture, respectively. $f_{@80}$ represents the time-domain frequency value having the maximum amplitude of the vibration that occurred while a finger scans a particular real texture with a speed of 80 mm/s.

In the first type, shown in (1), the vibration is spatially defined. In other words, the temporal frequency of the vibration (f) varies with finger velocity ($\dot{x}$) such that their multiplication is equal to the spatial frequency (f_s) of the corresponding surface. This modulation type most closely matches the frequency change expected while scanning a real texture with spatially distributed surface features. This modulation method is named frequency-modulation (FM) in the rest of the manuscript.

The second type of modulation, shown in (2), also modulates vibratory power with scanning velocity, but in a different way.

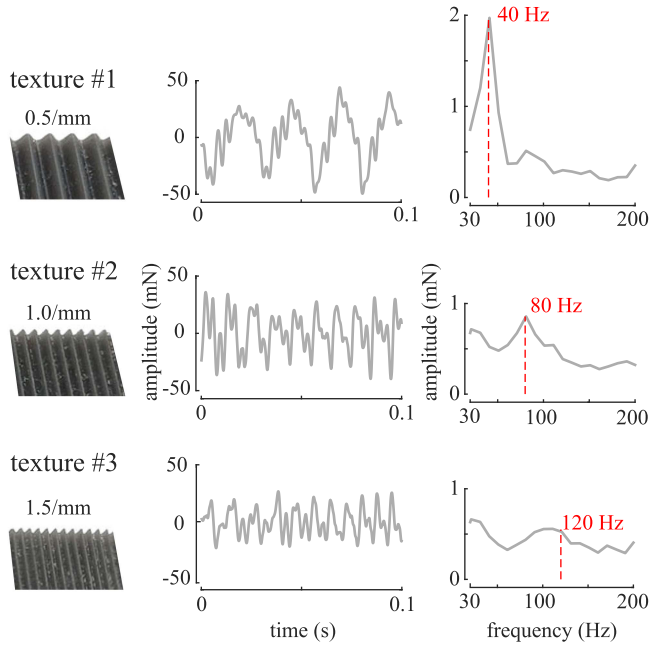

Fig. 3. Cropped photos of three real texture samples, all with different spatial frequencies but the same 1 mm height. To the left are shown the corresponding time and frequency domain responses of the lateral force between a finger and the texture measured while the finger moves over each surface with an average speed of 80 mm/s and normal force of 0.4 N. The expected temporal frequency corresponding to the spatial frequency scanned at 80 mm/s is indicated in red.

Here, we vary only the intensity of vibration with scanning velocity, while the temporal frequency ($f_{@80}$) remains unchanged at the peak component of the corresponding texture measured at 80 mm/s (check Fig. 3 for the values). In implementation, we proportionally increase the amplitude (A) linearly with increasing scanning speed from 0 to 80 mm/s; at faster scanning speeds, amplitude saturates at the same value used for the other modulation types. The particular speed threshold value at which amplitude no longer changes was somewhat arbitrary but was inspired by the plateauing of measured vibratory power at high speeds for real texture interactions [23]. We hereafter refer to this modulation type as amplitude-modulation (AM).

In contrast, the method in (3) demonstrates almost no speed dependence at all; a moving finger feels a sinusoidal vibration at the peak temporal frequency of the corresponding texture measured at 80 mm/s (Fig. 3) that does not change in frequency or amplitude, aside from turning off when the finger is completely still. This method is called no modulation (NM). All three types of modulation are graphically depicted in Fig. 2(c).

When choosing vibration amplitude, we sought to minimize intensity differences between the real textures and their virtual analogs to avoid overwhelming potentially more subtle differences in modulation type. Matching perceived intensities of texture-induced vibrations on the fingertip to vibrotactile vibrations applied on the base of the finger is non-trivial, especially across a large participant population, and outside the scope of this project. Instead, we chose to modulate virtual texture amplitudes between different frequencies to roughly the same ratios as seen in real texture force measurements in Fig. 3. Just as increasing the spatial frequency of a real texture reduces the peak forces on the fingertip (compare peak values in Fig. 3), increasing the frequency of our virtual textures reduces the driving voltage and therefore peak displacement of the actuator. For all real-to-virtual comparisons in this work, this ratio corresponds to 1, 1.5, and 2 V peak values for the high, mid, and low-frequency vibrations. Absolute maximum and minimum voltages were determined by the study authors, chosen to be perceptible yet not uncomfortably strong. Participants' amplitude preferences for each virtual texture frequency are further explored in the virtual-to-virtual texture comparisons.

We implemented velocity-dependent modulation of virtual textures using a NI PCIe-6323 DAQ and the Simulink Desktop Real-time environment. Finger position was sampled at 10 kHz, passed through a discrete derivative block and filtered (TC $=$ 0.01), and absolute valued to find finger speed. Position or speed determined actuator output as defined in (1)–(2). Finally, the input voltage of the actuator was filtered to obtain the desired displacement by accounting for actuator resonance. This procedure is summarized in Fig. 2(b)–(c).

III. Psychophysical Experiments

20 people (two left-handed, two women, ages 22–36) participated in this study. This study was approved by the Ethics Board of Delft University of Technology with case number 1781. All participants were students or employees of the university.

A. Training Procedure

Prior to each participant session, all experimental surfaces and the wearable ring were disinfected in accordance with approved coronavirus safety procedures. All participants were fitted with the wearable ring on their right index finger with a squeezing force of 0.5 N, and wore noise-canceling headphones playing continuous pink noise to mask potential sound effects from virtual texture actuation. The headphones also provided audio cues signaling the trial start and end times, as well as a metronomic beep during trials to ensure a consistent scanning speed across participants.

Applied Force: In order to reduce the effects of widely variable normal force, all participants practiced scanning a sample real texture for one minute while applying a 0.4 N pressing force to the surface. For this training, the sample texture was mounted on the force sensor (ATI Nano17 Titanium). During practice, they were provided with a visual graph of their real-time applied force.

Scanning Velocity: Subsequent to practicing controlling the contact force on real textures, participants practiced moving at a prescribed average scanning velocity for both real and virtual textures. The wearable ring was attached to the magnetic clip on the position tracking line, and participants practiced scanning real and virtual textures, both 50 mm in length while timing each 50 mm long swipe to a metronome beat played over the headphones. The metronome ensured a similar average scan velocity, in order to keep the temporal frequencies caused by real and spatially determined virtual textures similar across all participants. Following feedback from a pilot study, we chose an average swipe speed of 80 mm/s, which when paired with

the 50 mm texture length corresponds to a metronome speed of 96 bpm.

Free Magnitude Estimation: Finally, participants were guided through five practice trials comparing the coarsest real texture to virtual textures of various frequencies and modulation types, in order to become familiar with the similarity rating system. Each practice trial began with an "on" tone, then 30 seconds of metronome beats during which the participant could feel either texture, as long as their swipes were aligned with one texture length and a metronome period. At the end of the trial, an "off" tone played, and participants were instructed to provide a free magnitude estimation of the similarity between the pair. The rating for the first trial was arbitrary; subsequent trials that were less similar would be rated lower, and trials perceived as twice as similar as a previous pair should be rated twice as high. Ratings could be comprised of any non-zero positive number, including fractions. Participants could practice generating free magnitude estimations of similarity for more than 5 trials if they wished until both they and the experimenter agreed that they understood the concept.

TABLE I
EXPERIMENT 1 COMPARISONS

Trial #	Real texture	Virtual texture comparisons
1-3	low spatial freq.	low frequency (all modulation types)
4-5	low spatial freq.	medium and high frequency (only FM)
6-8	medium spatial freq.	medium frequency (all modulation types)
9-10	medium spatial freq.	low and high frequency (only FM)
11-13	high spatial freq.	high frequency (all modulation types)
14-15	high spatial freq.	low and medium frequency (only FM)

TABLE II
EXPERIMENT 2 COMPARISONS

Trial #	Pairwise Comparisons	Constant Parameters
1-3	Modulation type	Amplitude = medium, Spatial frequency = low
4-6	Modulation type	Amplitude = medium, Spatial frequency = high
7-9	Amplitude	Modulation = NM, Spatial frequency = low
10-12	Amplitude	Modulation = NM, Spatial frequency = high
13-15	Frequency	Amplitude = medium, Modulation = NM

B. Experiment 1: Virtual and Real Textures

The goal of Experiment 1 was to compare the similarity between real and virtual textures for different virtual modulation types, across different texture length scales, and contact conditions. In order to accommodate the large number of variables, we split this experiment into two 15-trial sets, performed before and after Experiment 2. The two sets differed only in contact conditions; for one set, participants felt all virtual textures while in contact with a 50 mm long flat surface printed in the same resin material as the real textured surfaces. For the other set, participants felt all virtual textures under non-contact conditions, in which their finger swiped over a 50 mm rectangular hole in the presentation plate (see Fig. 2(a)). Half of the participants performed the first set in contact and the second in non-contact, while for the other half the contact conditions were reversed. During the block of 15 trials, participants were instructed to consider the similarities between pairs of previous trials when evaluating the similarity between real and virtual textures in each subsequent trial. This approach ensured that participants' judgments remained consistent throughout each trial.

The 15 trials within each set were divided across the three real textures. The first five trials, presented in randomized order, compared the coarsest 0.5 mm^{-1} real texture to all three low-frequency virtual textures using each of the three modulation types, as well as all three frequency-modulated (FM) virtual textures. Note that the combination of the three modulation types for one frequency and three frequencies of one modulation type results in five total trials due to overlap between the two sets. The next five randomized trials consisted of the same type of comparisons, but with the real texture replaced with the 1 mm^{-1} sample, and the different modulation types replaced with the corresponding mid-frequency virtual textures. Similarly, the final five trials compared the finest 1.5 mm^{-1} real texture to the corresponding high-frequency virtual textures of all modulation types, along with all frequencies of FM virtual textures. Table I summarizes all the comparisons made in Experiment 1.

C. Experiment 2: Virtual Texture Comparison

For Experiment 2, participants once again made free magnitude estimations of similarity for texture pairs, but all textures were virtual and presented under non-contact conditions. In addition to rating similarity, participants were asked to indicate which texture was more "real", i.e. more similar to a real textured surface, and which was more "pleasant" to touch. In asking for judgments of pleasantness, we sought an additional qualitative measure of the virtual texture experience; in particular, we were curious if pleasantness mirrored judgments of realism. If participants perceived no realness or pleasantness differences, they were asked to choose a texture at random.

This experiment also consisted of 15 comparison trials, and both the trial order and left/right placement of each texture were randomized. Throughout the set, participants compared different modulation types to each other, different amplitudes to each other, and different frequencies to each other; see Table II and Section IV-D for details of the selected stimuli set.

D. Post-Experiment Questionnaire

Following Experiments 1, 2, and a repeat of Experiment 1 under the alternate contact condition, participants removed the wearable ring and answered a short survey. They were asked: "What made a virtual texture feel more or less like a real textured surface?" and "What made a virtual texture feel more or less pleasant?", as well as what effect contact or non-contact conditions for experiment 1 had on virtual texture perception.

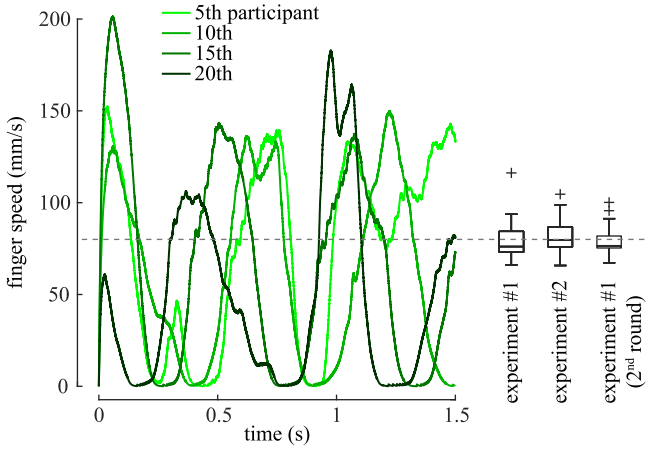

Fig. 4. Summary of participant scan speeds during all experimental rounds. The targeted speed of 80 mm/s is indicated with the dotted line. On the left, raw speed measurements are shown for four representative participants over several swipes. A summary of average speeds across all participants for each experiment is shown on the right.

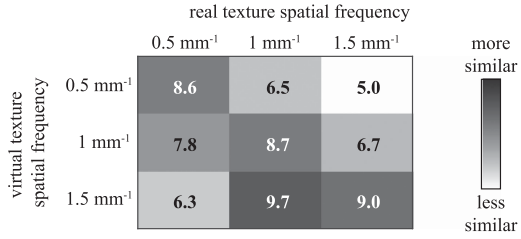

Fig. 5. Confusion matrix of rated similarities between real textures and frequency modulated virtual textures. Spatial frequencies of the virtual and real textures are indicated along the axes, and the normalized similarity ratings averaged across all participants and contact conditions are listed along with their corresponding levels of shading.

IV. Results

A. Scanning Speed

Standardizing scanning speed across participants was important to ensure uniformity of comparisons between a spatially determined real or virtual texture and a virtual texture in which the temporal frequency did not change. Fig. 4 summarizes the actual scanning speeds of participants throughout the experiments and confirms that average speeds were close to the desired 80 mm/s imposed by the metronome. Raw data from several participants in the first experiment highlights that actual velocities predictably varied quite widely during touch, as participants had to slow, stop, and turn around at the end of each swipe.

B. Participant Ratings

Since each participant created their own range of similarity ratings, we normalized similarity ratings across all participants for each 15-trial experimental block using geometric normalization procedure [27]. Accordingly, each participant's response was normalized by dividing by the participant's mean in the given experiment, then multiplying by the grand mean for all participants. Ratings were not normalized across the experimental blocks since each block consisted of substantially different conditions: virtual textures compared to either real stimuli or other virtual textures.

C. Virtual Textures Compared to Real Textures

We first investigated whether equivalent spatial frequencies resulted in higher similarity ratings between real and virtual texture pairs. We compared normalized similarity ratings for the subset of trials in which each spatially determined virtual texture (i.e., a frequency-modulated texture) was compared to each real texture. We first made a Shapiro-Wilk test and confirmed that all distributions passed the normality test. Then, we conducted a three-way ANOVA with repeated measures to test the effects of contact condition, real texture spatial frequency, and virtual texture spatial frequency on the similarity ratings.

The results showed that contact conditions did not significantly affect the perceived similarity of real and virtual textures ($F(1,19) = 0.002, p = 0.96$). However, both real ($F(2,38) = 7.8, p = 0.001$) and virtual ($F(2,38) = 18.51, p < 0.001$) texture spatial frequencies and their interaction ($F(4,76) = 32.53$, $p < 0.001$) significantly affected the similarity ratings. Fig. 5 shows the confusion matrix between real and virtual textures for the three spatial frequencies tested. The values represent the mean normalized similarity ratings across all participants and contact conditions. In general, participants rated equivalent spatial frequencies as more similar, and stimuli pairs were rated increasingly dissimilar as the frequencies increasingly differed. The highest frequency virtual texture was an exception to this trend, as it was consistently rated as more similar to the 1 mm^{-1} real sample.

Next, we investigated the impact of the modulation method on rated similarity, both for differing length scales and contact conditions. Similarity ratings between virtual and real texture pairs with equivalent spatial frequencies are summarized in Fig. 6; for AM and NM conditions, the assumed spatial frequency is the temporal frequency divided by the average scan speed of 80 mm/s. First, we confirmed that almost all distributions passed the normality assumption via a Shapiro-Wilk test. Then, using a three-way ANOVA with repeated measures, we assessed the significance of similarity differences caused by modulation type, spatial frequency, and contact condition.

The results revealed that contact conditions did not significantly affect the perceived similarities between real and virtual textures ($F(1,19 = 0.064,\ p = 0.804$). Nonetheless, the effects of modulation type ($F(2,38) = 8.16, p = 0.001$), spatial frequency ($F(2,38) = 6.03, p = 0.005$), and their interaction ($F(4,76) = 14.13,\ p = 0.007$) in the perceived similarities were statistically significant. Bonferroni corrected post hoc paired t-test showed that modulation type only had a significant impact on the similarity ratings at the lowest frequency; statistically different pairs ($p < 0.05$) are marked in Fig. 6.

D. Virtual Texture Comparisons

For the second set of experiments, participants compared different virtual textures to each other under non-contact conditions. Of these 15 trials, a subset was designed to compare

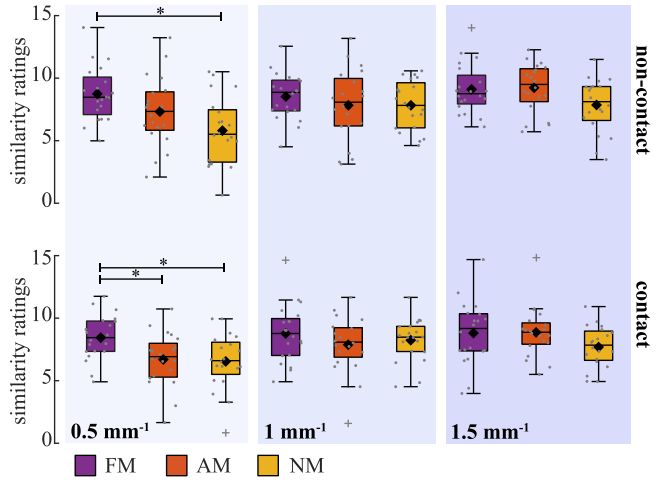

Fig. 6. Normalized similarity ratings between virtual and real texture pairs with equivalent spatial frequencies. The results corresponding to each experimental condition are color-coded. Individual participant responses and the mean are shown in gray and black dots, respectively, while box plots summarize the distribution. The central lines show the medians; box limits indicate the 25th and 75th percentiles. The whiskers extend to 1.5 times the interquartile range. Statistically significant pairwise comparisons ($p < 0.05$) are indicated with asterisks, $*$.

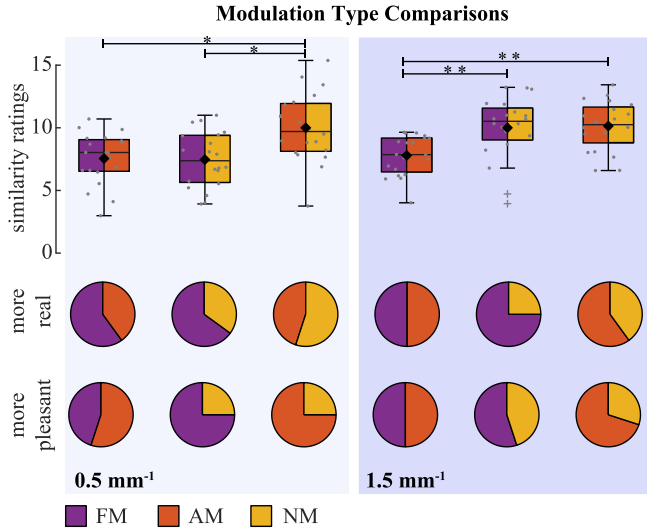

Fig. 7. Similarity ratings, realism, and pleasantness choices for pairs of virtual stimuli differed in modulation type (FM-AM, FM-NM, or AM-NM). All amplitudes were the medium value. The tested virtual texture spatial frequencies correspond to low or high values (0.5 mm^{-}1 or 1.5 mm^{-}1). The results corresponding to each experimental condition are color-coded. Individual participant responses and the mean are shown in gray and black dots, respectively, while box plots summarize the distribution. The central lines show the medians; box limits indicate the 25th and 75th percentiles. The whiskers extend to 1.5 times the interquartile range. Statistically significant pairwise comparisons are marked with asterisks; $*$ and $**$ mean $p < 0.05$ and $p < 0.01$, respectively.

modulation types, another to compare different amplitudes, and one to compare different frequencies. We first conducted Shapiro-Wilk tests and confirmed that almost all distributions passed the normality test. Then, we analyzed each subset separately using ANOVA with repeated measures and post hoc Bonferroni-corrected paired t-tests; the results are summarized below:

1) Modulation Comparisons: For six trials, study participants compared modulation types for both low frequency (0.5 mm^{-1}) and high frequency (1.5 mm^{-1}) virtual textures at the same amplitude (1.5 V). Normalized similarity ratings, realness, and pleasantness judgments are summarized in Fig. 7.

The results of two-way ANOVA with repeated measures revealed that compared modulation types ($F(2, 38) = 9.30$, $p < 0.001$) and texture frequency ($F(1, 19) = 7.39, p = 0.014$) significantly affected the perceived similarities, but there was no interaction between them ($F(2, 38) = 3.25$, $p = 0.05$). The significantly different pairs ($p < 0.05$ or $p < 0.01$) are depicted in Fig. 7. These differences are also reflected in trends across the two frequency conditions: for low-frequency texture pairs, AM and NM conditions were more similar to each other, while FM conditions were rated less similar to both. In contrast, for high-frequency textures, participants rated NM as similar to both FM and AM, but FM and AM were less similar to each other.

Pie charts indicate which percentage of participants selected one or the other texture as more real and pleasant; most strikingly, modulation of any type usually results in more realism and pleasantness than no modulation.

2) Amplitude Comparisons: Virtual textures (0.5 mm^{-1} and 1.5 mm^{-1}) with different amplitudes were also compared, keeping the modulation type the same (NM); see Fig. 8 for the summary of the results.

The results of two-way ANOVA with repeated measures showed that amplitude ($F(2, 38) = 22.91$, $p < 0.001$) and texture frequency ($F(1, 19) = 10.55$, $p = 0.004$) significantly affected the perceived similarities, but there was no interaction between them ($F(2, 38) = 0.114$, $p = 0.89$). The statistically significant pairwise comparisons ($p < 0.05$ or $p < 0.01$) are indicated in Fig. 8. Unsurprisingly, the greatest differences in amplitude result in the lowest similarity ratings.

For low-frequency virtual textures, the two higher amplitudes tended to be chosen as more realistic, with the medium amplitude found most pleasant. For high-frequency textures, the lowest amplitude was both more realistic and pleasant.

3) Frequency Comparisons: Only three trials compared textures of different frequencies, all at medium amplitude and NM; see Fig. 9 for the results.

A one-way ANOVA with repeated measures revealed that texture frequency significantly affected the perceived similarities ($F(2, 38) = 32.63$, $p < 0.001$). Statistically significant ($p < 0.001$) pairwise comparisons are marked in Fig 9. Similarly to amplitude comparisons, greater differences in frequency resulted in lower similarity ratings. Moreover, participants appeared to find the middle frequency more realistic than both higher and lower alternatives, and overwhelmingly more pleasant than the highest frequency.

E. Participant Feedback

Following the three experimental rounds, participants had a range of opinions on what improved the realism and pleasantness of virtual textures, but some common themes emerged: Six participants thought that the non-contact condition for virtual

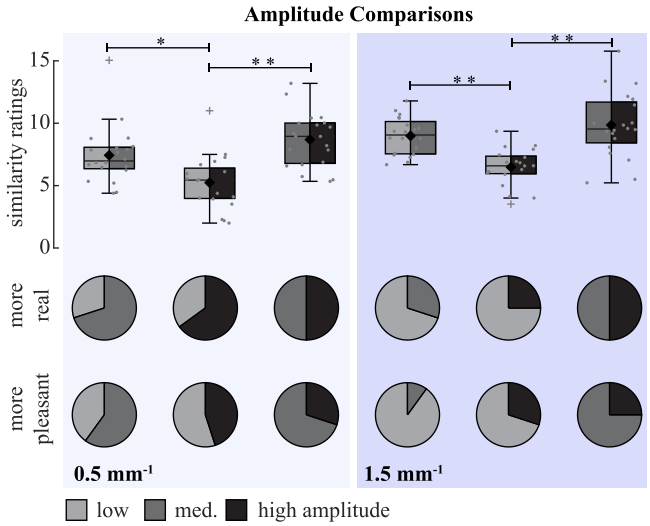

Fig. 8. Similarity ratings, realism, and pleasantness choices for pairs of virtual stimuli differed in amplitude (low-medium, low-high, or medium-high). No modulation was applied for these pairs. The tested virtual texture spatial frequencies correspond to low or high values (0.5 $mm^{-}1$ or 1.5 $mm^{-}1$). The results corresponding to each experimental condition are color-coded. Individual participant responses and the mean are shown in gray and black dots, respectively, while box plots summarize the distribution. The central lines show the medians; box limits indicate the 25th and 75th percentiles. The whiskers extend to 1.5 times the interquartile range. Statistically significant pairwise comparisons are marked with asterisks; $*$ and $**$ mean $p < 0.05$ and $p < 0.01$, respectively.

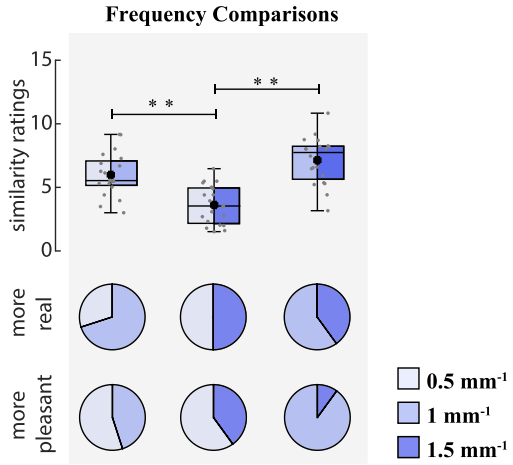

Fig. 9. Similarity ratings, realism and pleasantness choices for pairs of virtual stimuli differed in frequency (0.5-1 $mm^{-}1$, 0.5-1.5 $mm^{-}1$, or 1-1.5 $mm^{-}1$). All amplitudes were at the medium value, and no modulation was applied. The results corresponding to each experimental condition are color-coded. Individual participant responses and the mean are shown in gray and black dots, respectively, while box plots summarize the distribution. The central lines show the medians; box limits indicate the 25th and 75th percentiles. The whiskers extend to 1.5 times the interquartile range. Statistically significant ($p < 0.01$) pairwise comparisons are marked with asterisks $**$.

texture resulted in more realistic virtual texture rendering, some quite strongly, while 10 thought contact with a flat surface improved realism (the remaining were unsure or answered "depends"). A common reason for preferring non-contact was that the sensation of flat surface contact "clashed" with the actuation provided at the base of the finger, while those who preferred contact stated that the additional sensation on the fingertip helped. As over half the participants (12) commented on the effect of contact on realism unprompted early in the survey, this warrants further investigation.

V. Discussion

In this study, we investigated the effect of signal modulation methodology on the perceived realism of virtual textures rendered via a vibrotactile display stimulating the proximal phalanx of the index finger. For this aim, we first designed and characterized a ring-type wearable device. Then, we conducted psychophysical experiments in which 20 participants compared the perceived similarity of virtual textures generated via our device using three different modulation methodologies (FM, AM, and NM) to their 3D printed real counterparts. During the experiments, the participants explored the printed textures via their index fingertips; they felt the virtual ones by moving their index fingers on a smooth surface or in the air. Then in another psychophysical experiment, the same participants compared the similarity of virtual textures rendered via different modulation types and intensities. They also rated the perceived realism and pleasantness of the rendered textures.

A. Comparison of Virtual Textures to Their Real Counterparts

Our findings showed that using frequency modulation (FM) to render textures with a low spatial frequency significantly improved their perceived similarity to their real counterparts (check the first column in Fig. 6). Nonetheless, the modulation type did not make a perceptual difference when rendering textures at high spatial frequencies (compare columns in Fig. 6). Reduced sensitivity to modulation type at higher spatial frequencies may be due to differences in discrimination sensitivity at different frequencies [28]. Another reason could be the distinct mechanisms underlying the perception of coarse and fine textures. For example, previous research [29] showed that for coarse textures, both spatial deformation of the fingertip and the rate of change of these deformations play a role in their roughness perception; total vibratory power becomes more dominant for fine ones [30]. Earlier research conducted on a surface haptic display [31] showed evidence that due to these reasons, fine textures could be rendered by considering only a few highest components in their frequency spectrum, while coarser ones need more precision. Considering these studies, for rendering textures with low spatial frequencies, modifying the frequency of relocated vibrations similar to the fingertip vibrations might have helped participants better associate them with their real counterparts. However, the tested methodologies did not cause significant differences in vibration power, causing indifference to perceptual similarities for rendering fine textures.

Interestingly, exploring virtual textures on a flat surface having the same material or in the air by not making any contact did not make a significant difference when comparing them with their 3D printed counterparts (check Fig. 6). This result was unexpected because when humans interact with surfaces with their fingertips, they feel not only contact vibrations but also other properties, such as friction, thermal conductance, and stiffness, which the participants were deprived of in contactless conditions. Moreover, there is evidence in the literature [32], [33]

that remote vibrotactile stimulus can alter the perception of a real texture simultaneously encountered at the fingertip. The absence of measurable difference between our two contact conditions, despite these observed differences in the literature, could be due to several factors. One reason could be that the participants mainly relied on the vibration cues and ignored the others during the comparison test [34]. In fact, earlier studies [30] demonstrated that vibrations generated during fine texture exploration correlate with roughness perception, and roughness is one of the most dominant perceptual dimensions [35]. Another potential reason is the inconsistency across participant preference for one contact condition versus the other, as revealed by the post experiment questionnaire.

It is worth discussing here the implications of asking our participants to compare similarity of a real texture, felt on the glabrous skin of the fingertip, to a vibration applied to the hairy skin of the distal finger joint. Although not measured in our study, we expect that vibrations within our actuator's frequency range will easily travel the length of the entire finger to reach the other location; see [36] for a characterization of frequency-dependent wave propagation on the human hand. Amplitudes will diminish as vibrations propagate away from their source, but the single-frequency values used in this study will remain the same frequency. While these texture sensations applied at different locations are certainly not identical, they will engage a large and overlapping area of Pacinian mechanoreceptors. It would be interesting to observe participants' ability to make similarity judgements between texture-induced vibrations applied to locations with non-overlapping receptive fields, such as the fingertip and the wrist.

B. Comparison of Virtual Textures Between Each Other

When the participants compared the perceived realism of the different virtual textures, they felt the textures rendered via FM were more realistic than ones via AM and NM for both spatial frequencies (see Fig. 7). This result demonstrates that even though the textures were generated at a remote location, altering the frequency of the vibrations akin to ones occurring at the fingertip can generate noticeably more realistic textures. Nonetheless, for FM conditions, using higher amplitudes for rendering low spatial frequency textures led to more realistic rendering; however, this situation was the opposite for the ones with high spatial frequency (compare the pie charts in the first row in Fig. 8). This phenomenon is not surprising as the amplitude of the most dominant frequency component of the finger-contact vibrations that occur during interaction with 3D printed surfaces is highest at 40 Hz and lowest at 120 Hz (see Fig. 1).

Participants in aggregate appeared to find any type of modulation more pleasant than no modulation, across both frequencies and modulation types. Surprisingly, these preferences were present regardless of similarity ratings; despite FM and AM textures being rated as less similar than other modulation pairings, neither stands out as more pleasant than the other, yet both are consistently more often chosen as pleasant than NM textures. Participants may have disliked the abrupt changes in NM textures, and these findings suggest that any modulation is useful even if it does not enhance realism.

We found that the amplitude of the rendering signal significantly affects the perception of virtual textures with both low and high spatial frequencies. As anticipated, the similarity ratings for virtual-virtual texture comparisons were lowest when the amplitude differences were the highest (see Fig. 8). Amplitude also had an impact on perceived realism across frequencies; participants preferred higher displacement amplitudes for the lower frequencies and lower amplitudes for the higher frequencies. This is in line with the force amplitudes observed in Fig. 3 and the displacements used in Experiment 1. For all but one case, the virtual textures rendered with lower amplitude signals were perceived as more pleasant compared to the ones rendered with higher amplitude (compare the pie charts in the last row in Fig. 8).

C. Limitations and Future Directions

Virtual texture vibrations used in this study were very limited in their frequency content. While we chose single-frequency textures for simplicity and ease of modulation, most real textures are composed of much richer spectral information. It would be interesting to see if observed differences in virtual texture modulation extend to richer vibrations measured from real texture interactions. We were constrained from looking at higher-frequency textures due to a lack of a real texture that could produce a comparable and distinguishable high-frequency spectral component. We also could not look at lower-frequency textures due to the high pass filtering we used to protect our vibrotactile actuator from DC offsets.

The number of real textures (and their virtual analogs) in this study was also very limited, primarily due to our concerns about overall experimental length. Texture comparisons quickly become both mentally and physically exhausting, negatively impacting perceptual acuity and motivating us to keep our experimental sessions as short as possible. We believe that three spatial frequencies was the minimum number needed to observe initial trends in the perception of modulation types across frequency. However, our small number of textures, paired with the fact that they are all composed of single sinusoids, limits extrapolation of this study's results to all possible textures. Our current findings motivate future work exploring a wider range of textural frequency composition.

Our attempts to mitigate the perceptual impacts of amplitude differences were imperfect; the strength of texture-induced vibrations can vary considerably across participants and even individual trials, so we chose to simply set all vibration amplitudes to roughly similar ratios as that seen in measurements of real texture scans from the first author. Unintended differences in intensity almost certainly played a role in similarity ratings, particularly between pairs of stimuli that differed in frequency. Nonetheless, perceptual differences (or lack thereof) between modulation types within a single frequency and amplitude demonstrate that amplitude was certainly not the only factor in perceived similarity.

Finally, the wearable device and tracking system imposed additional limitations. The actuator was at the upper limit of usable size, stretching almost the full length of the distal phalanx for the average participant. This large size does not impede dexterity or hand closure, as it lies on the back of the hand while the securing strap wrapped around the finger was much narrower. However, users with particularly small hands could find the fit less comfortable if the actuator extends slightly past the first knuckle. We do not know the perceptual impact of our actuator applying vibrations laterally to the skin surface, or if actuation in the direction normal to skin surface (i.e., pressing into skin) might feel more realistic; our preliminary exploration with normal-direction actuators suggests they may result in more natural sensations. Additionally, when wearing the device, participants were limited to a small swipe range. This forced participants into somewhat unnaturally short movements, and future experimental setups may benefit from a larger workspace where participants may move more freely.

D. Conclusion

In summary, study participants were significantly more sensitive to differences in modulation type for the lowest frequency virtual textures than for those of higher frequency. For the lowest frequency textures, FM virtual textures were more similar to their real counterparts and less similar to virtual textures using other modulation types. In contrast, we saw no significant difference in similarity to higher frequency real textures for different modulation types. This suggests that preserving spatial frequency in texture rendering at finer length scales may not be necessary, at least for relocated actuation. This has the potential to simplify significantly signal design and modulation for relocated vibrotactile feedback in haptic texture rendering.

ACKNOWLEDGMENT

We acknowledge former M.Sc. student Sophia Huang (Northwestern University) for her preliminary investigations of amplitude-modulated vibrations for texture rendering, Michael Wiertlewski for allowing the laser doppler vibrometer in his lab as well as all the staff at 3Delft for their excitement and willingness to push their 3D printers to their spatial resolution limit. We also thank the anonymous reviewers whose valuable suggestions helped us improve this manuscript.

REFERENCES

[1] Meta, "Meta quest," 2022, Accessed: Aug. 4, 2022. [Online]. Available: https://store.facebook.com/quest

[2] HTC Corporation, "Vive," 2022, Accessed: Aug. 4, 2022. [Online]. Available: https://www.vive.com/us/

[3] HaptX Inc., "Haptx," 2022, Accessed: Aug. 4, 2022. [Online]. Available: https://haptX.com

[4] SenseGlove, "Senseglove," 2022, Accessed: Aug. 4, 2022. [Online]. Available: https://senseglove.com

[5] N. Zamani and H. Culbertson, "Effects of dental glove thickness on tactile perception through a tool," in *Proc. IEEE World Haptics Conf.*, 2019, pp. 187–192.

[6] D. Gueorguiev, B. Javot, A. Spiers, and K. J. Kuchenbecker, "Larger skin-surface contact through a fingertip wearable improves roughness perception," in *Proc. Int. Conf. Hum. Haptic Sens. Touch Enabled Comput. Appl.*, 2022, pp. 171–179.

[7] S.-Y. Teng, P. Li, R. Nith, J. Fonseca, and P. Lopes, "Touch&fold: A foldable haptic actuator for rendering touch in mixed reality," in *Proc. CHI Conf. Hum. Factors Comput. Syst.*, 2021, pp. 1–14.

[8] Z. Sun, M. Zhu, and C. Lee, "Augmented tactile-perception and haptic-feedback rings as human-machine interfaces aiming for immersive interactions," *Nature Commun.*, vol. 13, 2022, Art. no. 5224.

[9] C. Pacchierotti, G. Salvietti, I. Hussain, L. Meli, and D. Prattichizzo, "The hRing: A wearable haptic device to avoid occlusions in hand tracking," in *Proc. IEEE Haptics Symp.*, 2016, pp. 134–139.

[10] E. Pezent, P. Agarwal, J. Hartcher-O'Brien, N. Colonnese, and M. K. O'Malley, "Design, control, and psychophysics of tasbi: A force-controlled multimodal haptic bracelet," *IEEE Trans. Robot.*, vol. 38, no. 5, pp. 2962–2978, Oct. 2022.

[11] M. Sarac, T. M. Huh, H. Choi, M. R. Cutkosky, M. D. Luca, and A. M. Okamura, "Perceived intensities of normal and shear skin stimuli using a wearable haptic bracelet," *IEEE Robot. Automat. Lett.*, vol. 7, no. 3, pp. 6099–6106, Jul. 2022.

[12] H. Culbertson, J. Unwin, and K. J. Kuchenbecker, "Modeling and rendering realistic textures from unconstrained tool-surface interactions," *IEEE Trans. Haptics*, vol. 7, no. 3, pp. 381–393, Jul.-Sep. 2014.

[13] H. Culbertson and K. J. Kuchenbecker, "Ungrounded haptic augmented reality system for displaying roughness and friction," *IEEE/ASME Trans. Mechatron.*, vol. 22, no. 4, pp. 1839–1849, Aug. 2017.

[14] B. L. Kodak and Y. Vardar, "FeelPen: A haptic stylus displaying multimodal texture feels on touchscreens," 2022. [Online]. Available: https://www.techrxiv.org/articles/preprint/FeelPen_A_Haptic_Stylus_Displaying_Multimodal_Texture_Feels_on_Touchscreens/21341871

[15] A. İşleyen, Y. Vardar, and C. Basdogan, "Tactile roughness perception of virtual gratings by electrovibration," *IEEE Trans. Haptics*, vol. 13, no. 3, pp. 562–570, Jul.-Sep. 2020.

[16] R. F. Friesen, R. L. Klatzky, M. A. Peshkin, and J. E. Colgate, "Building a navigable fine texture design space," *IEEE Trans. Haptics*, vol. 14, no. 4, pp. 897–906, Oct.-Dec. 2021.

[17] C. Bernard, J. Monnoyer, and M. Wiertlewski, "Harmonious textures: The perceptual dimensions of synthetic sinusoidal gratings," in *Proc. Int. Conf. Hum. Haptic Sens. Touch Enabled Comput. Appl.*, 2018, pp. 685–695.

[18] C. Gaudeni, L. Meli, L. A. Jones, and D. Prattichizzo, "Presenting surface features using a haptic ring: A psychophysical study on relocating vibrotactile feedback," *IEEE Trans. haptics*, vol. 12, no. 4, pp. 428–437, Oct.-Dec. 2019.

[19] J. Saint-Aubert, "Identifying tactors locations on the proximal phalanx of the finger for navigation," in *Proc. Int. Conf. Hum. Haptic Sens. Touch Enabled Comput. Appl.*, 2020, pp. 42–50.

[20] A. Talhan, H. Kim, and S. Jeon, "Tactile ring: Multi-mode finger-worn soft actuator for rich haptic feedback," *IEEE Access*, vol. 8, pp. 957–966, 2020.

[21] O. Ariza, P. Lubos, F. Steinicke, and G. Bruder, "Ring-shaped haptic device with vibrotactile feedback patterns to support natural spatial interaction," in *Proc. 25th Int. Conf. Artif. Reality Telexistence, 20th Eurograph. Symp. Virtual Environments*, 2015, pp. 175–181.

[22] L. R. Manfredi et al., "Natural scenes in tactile texture," *J. Neuriophysiol.*, vol. 111, no. 9, pp. 1792–1802, 2014.

[23] C. M. Greenspon, K. R. McLellan, J. D. Lieber, and S. J. Bensmaia, "Effect of scanning speed on texture-elicited vibrations," *J. Roy. Soc. Interface*, vol. 17, no. 167, 2020, Art. no. 20190892.

[24] E. Vezzoli, T. Sednaoui, M. Amberg, F. Giraud, and B. Lemaire-Semail, "Texture rendering strategies with a high fidelity-capacitive visual-haptic friction control device," in *Proc. Int. Conf. Hum. Haptic Sens. Touch Enabled Comput. Appl.*, 2016, pp. 251–260.

[25] W. McMahan and K. J. Kuchenbecker, "Dynamic modeling and control of voice-coil actuators for high-fidelity display of haptic vibrations," in *Proc. IEEE Haptics Symp.*, 2014, pp. 115–122.

[26] S. J. Lederman and R. L. Klatzky, "Haptic perception: A tutorial," *Attention Percep. Psychophys.*, vol. 71, no. 7, pp. 1439–1459, 2009.

[27] A. M. Murray, R. L. Klatzky, and P. K. Khosla, "Psychophysical characterization and testbed validation of a wearable vibrotactile glove for telemanipulation," *Presence: Teleoperators Virtual Environments*, vol. 12, no. 2, pp. 156–182, 2003.

[28] A. Israr, H. Z. Tan, and C. M. Reed, "Frequency and amplitude discrimination along the kinestheticcutaneous continuum in the presence of masking stimuli," *J. Acoustical Soc. Amer.*, vol. 120, pp. 2789–2800, 2006.

[29] A. Smith, C. Chapman, M. Deslandes, J. Langlais, and T. MP, "Role of friction and tangential force variation in the subjective scaling of tactile roughness," *Exp. Brain Res.*, vol. 144, no. 2, pp. 211–23, 2002.

[30] S. Bensmaia and M. Hollins, "The vibrations of texture," *Somatosensory Motor Res.*, vol. 20, no. 1, pp. 33–43, 2003.
[31] T. Fiedler and Y. Vardar, "A novel texture rendering approach for electrostatic displays," in *Proc. Int. Workshop Haptic Audio Interaction Des.*, 2019.
[32] M. Jamalzadeh, B. Güçlü, Y. Vardar, and C. Basdogan, "Effect of remote masking on detection of electrovibration," in *Proc. IEEE World Haptics Conf.*, Tokyo, Japan, 2019, pp. 229–234.
[33] R. T. Verrillo and B. G. Calman, "Masking of vibrotactile sensations from a remote site," *J. Acoustical Soc. Amer.*, vol. 69, 1998, Art. no. S23.
[34] B. Richardson, Y. Vardar, C. Wallraven, and K. J. Kuchenbecker, "Learning to feel textures: Predicting perceptual similarities from unconstrained finger-surface interactions," *IEEE Trans. Haptics*, vol. 15, no. 4, pp. 705–717, Oct.-Dec. 2022.
[35] S. Okamoto, H. Nagano, and Y. Yamada, "Psychophysical dimensions of tactile perception of textures," *IEEE Trans. Haptics*, vol. 6, no. 1, pp. 81–93, First Quarter 2013.
[36] B. Dandu, Y. Shao, A. Stanley, and Y. Visell, "Spatiotemporal haptic effects from a single actuator via spectral control of cutaneous wave propagation," in *Proc. IEEE World Haptics Conf.*, 2019, pp. 425–430.

Rebecca Fenton Friesen (Member, IEEE) received the Ph.D. degree in mechanical engineering from Northwestern University, Evanston, IL, USA, in 2020. In 2022, she joined Texas A&M University, College Station, TX, USA, as an Assistant Professor of Mechanical Engineering. She was a Postdoc with the Cognitive Robotics Department with the Delft University of Technology, Delft, The Netherlands. Her work is centered on surface haptic actuation and perception, particularly for wide bandwidth virtual texture rendering.

Yasemin Vardar (Member, IEEE) received the Ph.D. degree in mechanical engineering from Koç University, Turkey in 2018. She is an Assistant Professor with the Delft University of Technology, Delft, the Netherlands. She completed her Postdoctoral Research with the Max Planck Institute (MPI) for Intelligent Systems in Stuttgart, Germany, till 2020. Her research interests include human tactile perception and haptic interfaces. She was the recipient of the 2021 NWO VENI Grant, 2018 Eurohaptics Best Ph.D. Thesis Award, IEEE WHC 2017 Best Poster Presentation Award, and TUBITAK Ph.D. Fellowship. She was selected for the 2019 MPI Sign Up! Career-building Program. She is currently the Co-chair of the Technical Committee on Haptics.